Effect of Land Surface Variation on Precipitation over Asian Monsoon Region

Akira Kawabata and * Kazuhisa Tsuboki
Hydrospheric Atmospheric Research Center, Nagoya University,
Furo-cho, Chikusa-ku, Nagoya, 464-8601 Japan
Phone: +81-52-789-3494, Fax: +81-52-789-3436
E-mail: kawabata@ihas.nagoya-u.ac.jp, tsuboki@ihas.nagoya-u.ac.jp

1. Introduction

Evapotranspiration is one of the key land surface processes that regulate climate systems, because it not only provides the atmosphere with water vapor but also determines temperature near the surface via the ratio between sensible and latent heat fluxes. Various researches into understanding the effect of the land surface evapotranspiration on the atmospheric water circulation have been carried out (e.g. Shukla and Mintz (1982)), however, the impacts and physical processes are still poorly understood.

To investigate this problem, eastern Asia significantly influenced by summer monsoon is an interesting subject. Over this region, a large amount of rainfall is brought by the stationary Baiu front, which appears from eastern China to Japan. Evapotranspiration from the land surface is also abundant, since characteristic land cover, such as paddy fields around the Huaihe river basin, widely spreads (Fig. 1). Moreover, Kitoh (2000) conducted a numerical experiment by general circulation model (GCM), and suggested that land surface conditions are crucial for the atmospheric water circulation over eastern Asia.

In this study, two kinds of numerical simulations were conducted with a regional atmospheric model to investigate the impact of change in land surface evapotranspiration on the atmospheric water circulation, especially in terms of precipitation, and its physical processes.

2. Numerical model and experimental design

The Japan Spectral Model (JSM; Segami et al. 1989) was employed for the numerical experiments in the present study. The model has 129×129 grids with 90 km horizontal spacing and 23 vertical layers. The model and analysis domains are shown in Fig. 1.

In the calculation, evapotranspiration from the land and sea surfaces is estimated using following equation.

$$E = - \rho C_h |V_a| \beta \{q_a - q_{sat}(T_s)\}$$

To introduce the realistic spatial variation of moisture availability β, 94 types of land cover classification data provided by U.S. Geological Survey (Loveland et al. 2000) were rearranged into 9 types for simplicity. The values of β as well as roughness z_0 for each land cover class, derived from some literature (e.g., Kondo (1994)), were determined as shown in Table 1.

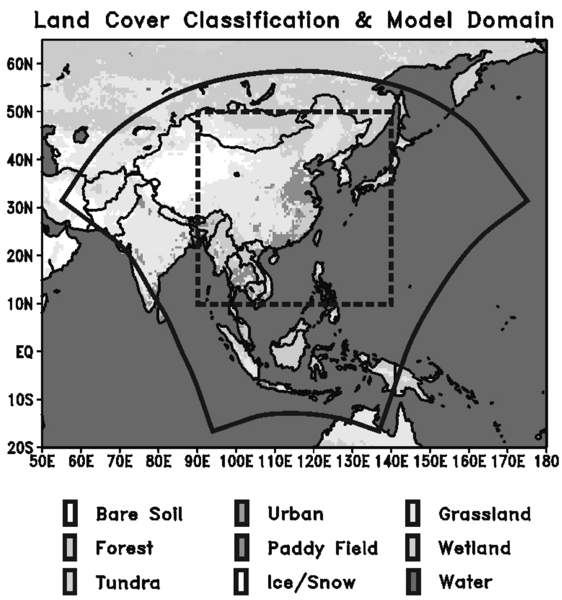

Fig. 1. Distribution of land cover classification. Solid and broken lines indicate model and analysis domains, respectively.

Two calculations were performed for 1 month from June 1 to 30, 1998, when the GEWEX Asian Monsoon Experiment-Intensive Observation Period (GAME-IOP) was carried out (Yasunari 1998). The simulations were evaluated using the results from June 6 to 30, because the first 5 days were considered as spin-up time and not utilized. First, the Standard simulation with the realistic spatial distribution of β was conducted to verify whether JSM was able to simulate fundamental features of atmospheric water circulation. Second, the calculation named NoLE, for no land surface evapotranspiration, was carried out to be compared with the results of the Standard simulation and investigate the impact of the land surface evapotranspiration decrease on precipitation and atmospheric conditions. In the both simulations, the initial and boundary conditions were supplied by the GAME reanalysis data every 6 hours (Yamazaki et al. 2000). For the sea surface, the same conditions were used, that is, the sea surface temperature was estimated from the climatic monthly mean data, and β was set to 1.00. Accordingly, the only difference between the both calculations was the values of β over the land area.

3. Results and discussion

3.1 Standard simulation

The simulated precipitation and horizontal wind at 850 hPa from June 6 to 30 with the realistic spatial variation of β are shown in Fig. 2. The CPC (Climate Prediction Center) Merged Analysis of Precipitation (CMAP; Xie and Arkin 1997) data and the reanalysis horizontal wind data are also shown in Fig. 3. From southeastern China to Japan, a rainfall zone brought by the Baiu front is simulated as in CMAP data, although the width of the precipitation belt is narrower. The westerly low level jet (LLJ), which is one of the features in the summer Asian monsoon region, appears from the Bay of Bengal and merges with the southeasterly flow along the periphery of the subtropical high. It agrees well with the reanalysis data. As for other atmospheric conditions such as sea level pressure, the simulation is similar with the reanalysis data. Thus JSM can simulate the basic characteristics of atmospheric water circulation for this period.

Category	Moisture Availability (β)	Roughness (z_0) [m]
Bare Soil	0.00	0.0001
Urban	0.05	3
Grassland	0.20	0.2
Forest	0.30	0.7
Paddy Field	0.60	0.05
Wetland	0.40	0.1
Tundra	0.40	0.01
Ice/Snow	1.05	0.005
Water	1.00	0.0002

Table 1. Values of moisture availability and roughness for each land cover classification.

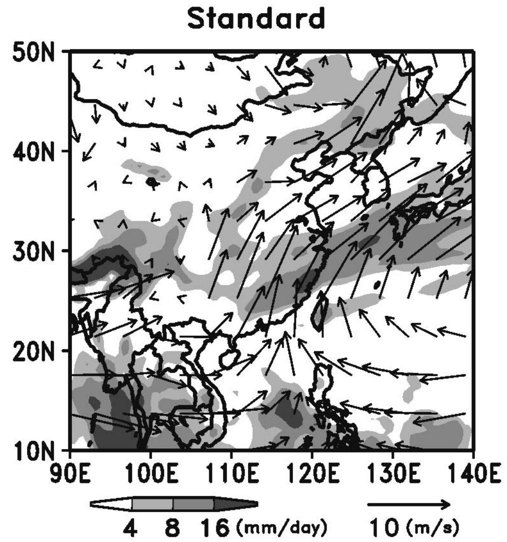

Fig. 2. 25-day averaged precipitation and horizontal wind at 850 hPa calculated by the Standard simulation.

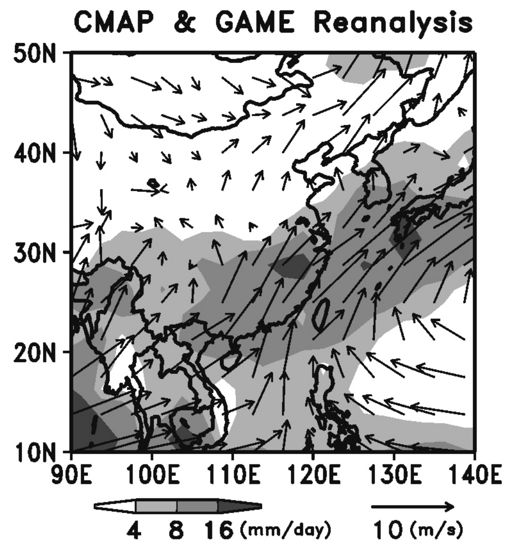

Fig. 3. Same as Fig. 2, but for the CMAP data for precipitation and the GAME reanalysis data for horizontal wind.

3.2 NoLE simulation

Figure 4 shows the calculated precipitation by the NoLE simulation with no evapotranspiration from the land surface. The rainfall zone corresponding to the Baiu front is found as in the Standard simulation. To evaluate effects on the rainfall amount of the evapotranspiration cut off over the land area quantitatively, 10-degree averaged differences in precipitation for the NoLE - Standard simulations focusing on eastern China are shown in Fig. 5. The precipitation decrease reaches approximately 1 mm/day (20% to 40% in comparison with the Standard simulation) over Region A, however, the rainfall amount is almost unchanged (about 1% decrease) over Region B.

In Fig. 6, difference in specific humidity at the surface is shown. In the NoLE simulation, the specific humidity is significantly decreased over Region A, while the difference is less than 10% over Region B as in rainfall. Figure 7 shows differences in lower horizontal wind and sea level pressure. The southerly wind component of LLJ in the NoLE simulation is intensified along the inside of the coastline due to the pressure depression appeared over the continent. This enhanced wind supplies larger amount of water vapor to the lower atmosphere, and the increase in horizontal water vapor flux compensates for the land surface evapotranspiration cut off over Region B. On the other hand, the increase is small in comparison to the evapotranspiration decrease over Region A. In Fig. 8, difference in surface temperature for the NoLE - Standard simulations is shown. The temperature in the NoLE simulation is 1 to 4 degrees higher over the area where the pressure depression is found in Fig. 7. This increase in temperature results from heating of the lower atmosphere by sensible heat, and brings the pressure depression.

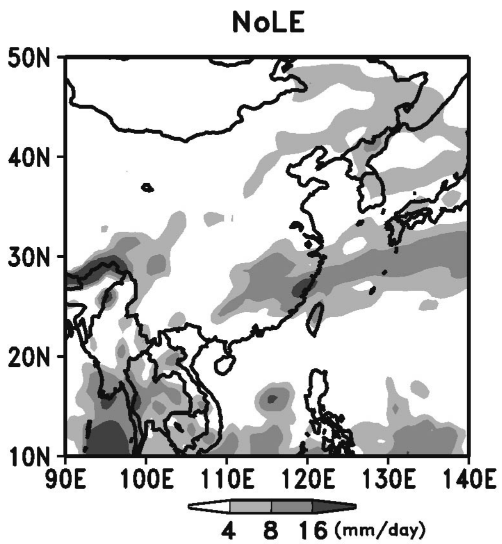

Fig. 4. 25-day averaged precipitation calculated by the NoLE simulation.

4. Conclusion

Numerical simulations with a regional atmospheric model were carried out to evaluate how the change in the land surface evapotranspiration affects atmospheric

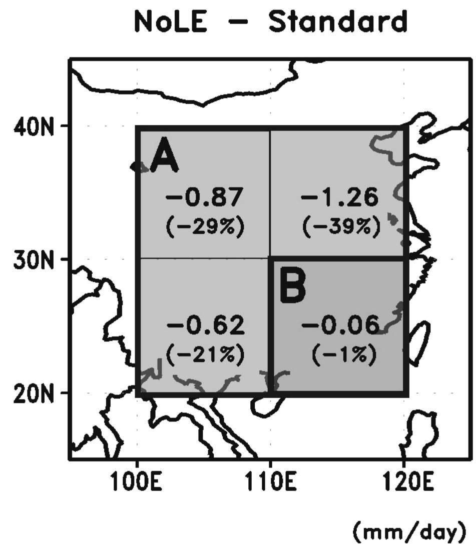

Fig. 5. 10-degree averaged difference in simulated 25-day averaged rainfall amount for the NoLE - Standard simulations over eastern China.

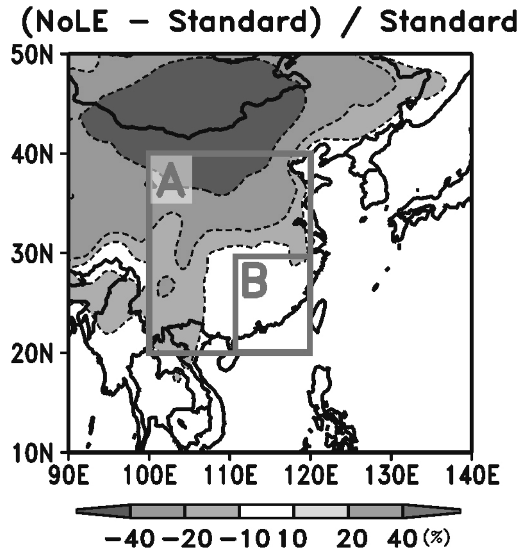

Fig. 6. Difference in 25-avaraged specific humidity at the surface for the NoLE - Standard simulations in comparison with the Standard simulation.

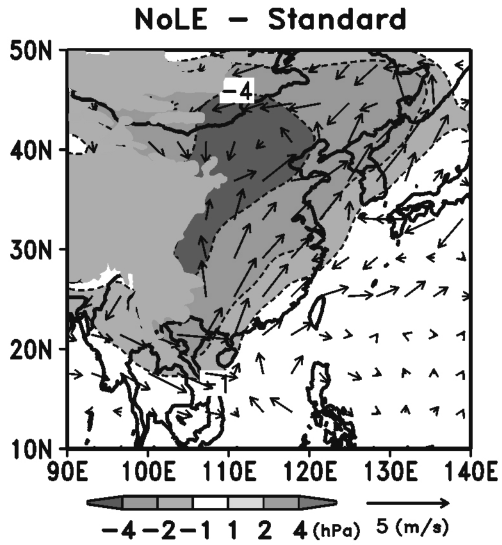

Fig. 7. Differences in 25-avaraged horizontal wind at 850 hPa and sea level pressure for the NoLE - Standard simulations. Areas with mountains of more than 1500 m are shadowed.

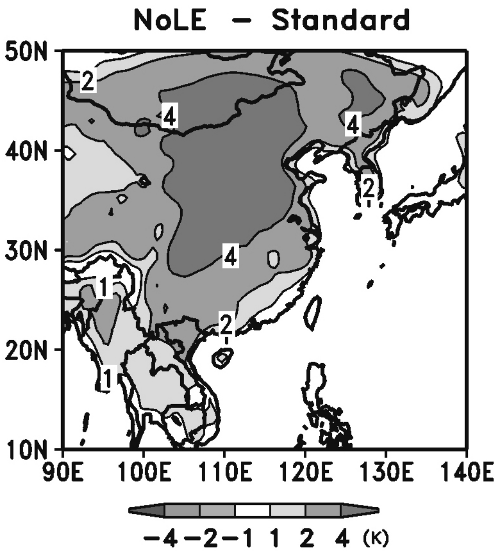

Fig. 8. Difference in 25-day averaged surface temperature for the NoLE - Standard simulations.

water circulation, especially focusing on precipitation.

The NoLE simulation with no evapotranspiration from the land surface was conducted to be compared with the results of the Standard simulation, and two regions were identified in terms of difference in rainfall amount. Over Region A, the decrease in the rainfall amount was significant because the effect of no evapotranspiration from the land surface was dominant. In contrast, the rainfall amount was almost unchanged in spite of no land surface evapotranspiration over Region B, because the decrease in moisture due to a lack of land surface evapotranspiration was compensated by the enhanced horizontal water vapor flux induced by lower atmosphere heating by sensible heat.

The differences that regulate the effects of the land surface evapotranspiration are considered to depend on the location of the moisture source, such as oceans, and the airflow systems which transport water vapor.

Acknowledgments

We acknowledge the GAME reanalysis project conducted by the Meteorological Research Institute, Japan Meteorological Agency and Earth Observation Research Center/ National Space Development Agency of Japan for the reanalysis data. We are also grateful to USGS - NASA Distributed Active Archive Center for the land cover classification data. Special thanks are also expressed to Dr. Hiyama for his discussions and assistance in land surface processes.

References

Kitoh, A., 2000: *Proc. of The Twenty-Fifth Annual Climate Diagnostics And Prediction Workshop*, 242-245.

Kondo, J., 1994: Meteorology of the water environment -water and heat balance of the earth's surface-. Asakura Press, 348pp (in Japanese).

Loveland, T. R., B. C. Reed, J. F. Brown, D. O.Ohlen, J. Zhu, L.Yang and J. W. Merchant, 2000: *Int. J. Remote Sens.*, **21**, 1303-1330.

Segami, A., K. Kurihara, H. Nakamura, M. Ueno, I. Takano and Y. Tatsumi, 1989: *J. Meteor. Soc. Japan*, **67**, 907-924.

Shukla, J. and Y. Mintz, 1982: *Science*, **215**, 1498-1501.

Xie, P. and P. A. Arkin, 1997: *Bull. Amer. Meteor. Soc.*, **78**, 2539-2558.

Yamazaki, N., H. Kamahori, A. Yatagai, K. Takahashi, H. Ueda, K. Aonashi, K. Kuma, Y. Takeuchi, H. Tada, Y. Fukutomi, H. Igarashi, H. Fujinami and Y. Kajikawa, 2000: *Tenki*, **47**, 659-663 (in Japanese).

Yasunari, T., 1998: *Tenki*, **45**, 501-514 (in Japanese).